RESOLVED TIME DIFFERENCE BETWEEN CALCIUM-ALUMINUM-RICH INCLUSIONS AND THEIR WARK LOVERING RIMS INFERRED FROM Al-Mg CHRONOLOGY OF TWO INCLUSIONS FROM A CV3 CARBONACEOUS CHONDRITE. P. Mane[1], M. Bose[2], and M. Wadhwa[1]. [1]School of Earth and Space Exploration, Arizona State University, Tempe, AZ 85287. (Prajkta.Mane@asu.edu). [2]Department of Chemistry and Biochemistry, Arizona State University, Tempe, AZ 85287.

Introduction: The refractory Calcium-Aluminum-rich Inclusions (CAIs) preserve petrographic and geochemical records of the earliest events that shaped our Solar System. Absolute high-resolution Pb-Pb dating of CAIs has revealed them to be the oldest solids in the Solar System [1-4]. Another useful high-resolution relative dating technique is the ^{26}Al-^{26}Mg short-lived chronometer which has been used extensively for relative dating of these early Solar System objects (e.g., [5-7]). CAIs typically exhibit multiple mono- or bi-mineralic layered rim sequences, which are termed as Wark-Lovering (WL) rims [8]. As such, these rim sequences represent unique yet universal event(s) in the early Solar System. The WL rims are made of refractory minerals such as hibonites, spinels, perovskites, melilites, and Al-rich pyroxenes; alteration phases such as nepheline, anorthite, sodalite, grossular and wollastonite have also been reported in these rim sequences [9-11].

Based on their refractory element composition, WL rims were considered to be a consequence of flash heating (>2500 K temperatures for <2 s time interval) and were argued to represent the evaporation residues from such events [12]. However, textural studies through high spatial resolution Focused Ion Beam Transmission Electron Microscopy (FIB TEM) analyses of WL rims show a complex mixture of polycrystalline material, and the presence of triple junctions and subhedral grains suggest formation from melt. This has been considered as evidence for flash heating caused by mechanisms such as shock waves [11, 13-15]. The variation in the stable isotope fractionation of Mg in the rims suggest that they formed at a partial pressure of Mg approaching saturation (unlike the CAI interiors) and based on this observation it has been suggested that these rim were formed by condensation [17]. Many oxygen isotopic analyses of WL rims show ^{16}O enrichment (similar to the CAI parent reservoir) as well as the presence of a ^{16}O-poor component. Both these components are present within the same rim sequence [9-10, 17, 19]. These variations in oxygen isotopes have been explained by flash heating and subsequent re-equilibration with nebular gas [9, 15] or condensation processes rims forming from different O isotopic nebular reservoirs [15, 21].

Constraints on the relative time difference between initial CAI formation and WL rim formation will help to identify the appropriate model for the rim sequence formation and will also provide a better understanding of the processes and dynamics within the protoplanetary disk. However, since the thickness of the individual layers in the rims is barely a few microns, it poses a challenge in analyzing these mineral layers using traditional mass spectrometry techniques. Only a few ion microprobe analyses of Al-Mg systematics in WL rim sequences have been conducted so far, and these suggest formation several hundred thousand years after CAI formation [16-18].

In this study, we present high spatial resolution Al-Mg chronology of CAIs and their rims using a NanoSIMS instrument. Specifically, we analyzed two CAIs and their WL rims from the Northwest Africa (NWA) 8323 CV3 carbonaceous chondrites in order to determine the time difference between the formation of

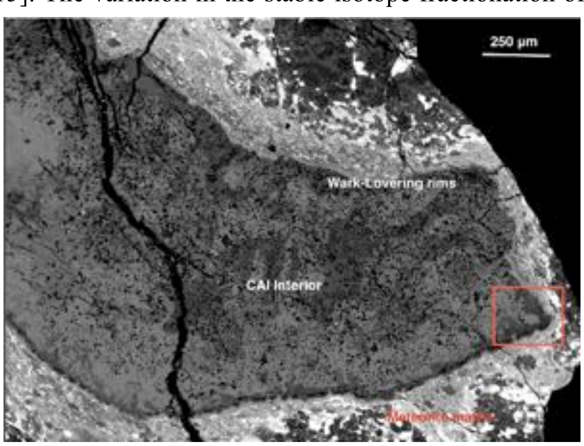

Figure 1: Back Scattered Electron (BSE) image of CAI-2.

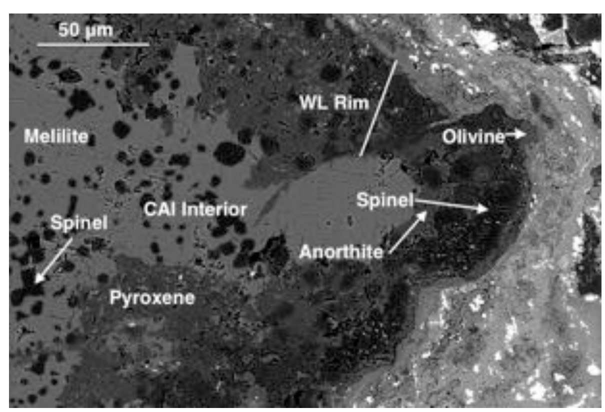

Figure 2: Back Scattered Electron (BSE) image of WL rim sequence of CAI-2. This region is shown in a red box on Fig. 1.

CAIs and their WL rims.

Analytical Methods: The characterization of the mineralogy of CAIs and their WL rim sequences was done using the new JEOL JXA-8530F electron microprobe at Arizona State University (ASU). Magnesium isotope analyses were conducted using a Cameca NanoSIMS 50L at ASU. A 16 keV O^- primary beam at ~20-30 pA current was rastered over 5 × 5 μm areas on the sample (dwell time of 1 ms/pixel with 256^2 pixels). Positive secondary ion signals for $^{24}Mg^+$, $^{25}Mg^+$, $^{26}Mg^+$ and $^{27}Al^+$ were collected simultaneously using electron multipliers from the central 2.5 × 2.5 μm area. Isobaric interferences such as ^{23}NaH, $^{12}C_2$, ^{24}MgH, $^{13}C_2$, and $^{12}C^{14}N$ are completely resolved using a mass resolving power of ~9000. The raw ratios were corrected for dead time and instrumental mass bias using terrestrial standards. Analysis time varied between 30-90 minutes per spot for different mineral phases. Both natural and instrumental mass fractionation were corrected using an exponential law with β = 0.514. Radiogenic ^{26}Mg excess ($\delta^{26}Mg^*$) is expressed in per mil unit with respect to terrestrial standards. The uncertainties reported here are from counting statistical error (2 sigma). San Carlos olivine and augite, Lake County plagioclase, NIST 610 synthetic glass and BCR-2 glass were used as terrestrial standards. San Carlos olivine shows external reproducibility (2SD) of $\delta^{26}Mg^*$ of ±4.7‰ (n = 12), whereas Lake County plagioclase shows external reproducibility (2SD) of ±23‰ (n = 3).

Sample Description: NWA 8323 is an oxidized CV3 carbonaceous chondrite, with a low shock grade as well as low weathering grade [21]. CAI-1 is a coarse-grained inclusion consisting of melilite, spinel, anorthite and pyroxene. The WL rim sequence consist of olivine, spinel, and anorthite. CAI-2 is similarly a coarse-grained inclusion that is made up of spinel, anorthite, Ti-rich pyroxene, and melilite. This inclusion also contains some Fe-Ni metal. The WL rim sequence consists of anorthite, spinel, pyroxene and some patchy occurrence of nepheline (Figs. 1 and 2).

Results and Discussion: Fig. 3 shows Al-Mg isochrons for CAI-1, and its WL rim. The interior of the CAI shows an initial $^{26}Al/^{27}Al$ ratio of (5.2 ± 1.6) × 10^{-5} (with initial $\delta^{26}Mg^*$ of 1 ± 7‰; MSWD = 0.8). In the WL rim for this CAI, only an upper limit on the initial $^{26}Al/^{27}Al$ ratio of <2.0 × 10^{-5} can be determined. As such, the minimum time between formation of CAI-1 and its WL rims is ~590,000 years. Fig. 4 shows Al-Mg isochrons for CAI-2, and its WL rim. The interior of the CAI shows initial $^{26}Al/^{27}Al$ ratio of (4.7 ± 1.2) × 10^{-5} (with $\delta^{26}Mg^*$ intercept of 6 ± 12‰; MSWD = 0.1). In the WL rim for this CAI, only an upper limit on the initial $^{26}Al/^{27}Al$ ratio of <1.8 × 10^{-5} can be determined. Therefore, the minimum time difference between the formation of CAI-2 and its WL rims is ~690,000 years. The difference in time of formation between the CAIs and their WL rims, defined by these two inclusions is at least twice than reported by previous studies [14, 16-17]. This implies that CAIs were likely not accreted into parent bodies for at least this duration of time, which has significant implications for nebular dynamics.

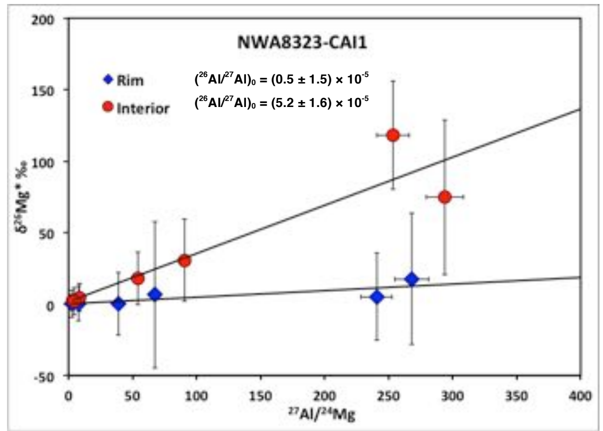

Figure 3: Al-Mg isochron of CAI-1 and its WL rim.

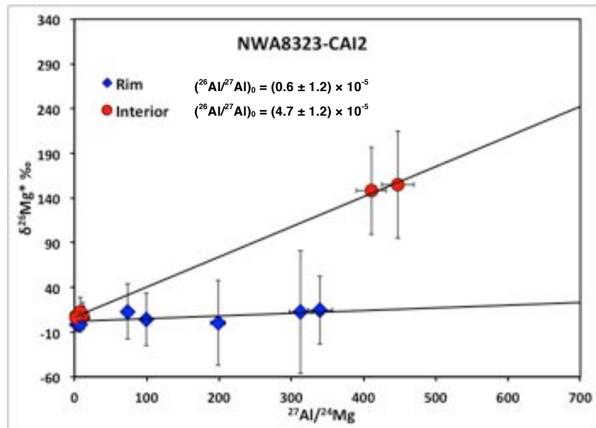

Figure 4: Al-Mg isochron of CAI-4 and its WL rim.

References: [1] Amelin Y. et al. (2002) *Science, 297*, 1678-1683. [2] Amelin Y. et al. (2009) *GCA, 73*, 5212-5223. [3] Bouvier A. and Wadhwa M. (2010) *Nature Geosci., 3*, 637-641. [4] Connelly J. N. et al. (2012) *Science, 338*, 651-655. [5] MacPherson G. et al. (1995) *Meteoritics, 30*, 365-386. [6] Bizzarro M. et al. (2004) *Nature, 431*, 275-278. [7] Jacobsen B. et al. (2008) *EPSL, 272*, 353-364. [8] Wark D. A. & Lovering J. F. (1977) *LPSC IIX, 95-112.* [9] Hirai K. et al. (2002) *LPSC XXXIII,* Abstract #1419. [10] Yoshitake M. et al. (2002) *LPSC XXXIII,* Abstract #1502. [11] Zega T. J. et al. (2007) *MAPS, 42*, 5289. [12] Wark D. A. & Boynton W. V. (2001) *MAPS, 36*, 1135-1166. [13] Toppani A. et al. (2006) *LPSC XXXVII,* Abstract #2030. [14] Stroud R. M. at al. (2007) *Workshop on the Chronology of Meteorites and the Early Solar System,* #1374. [15] Ito M. & Messenger S. (2010) *MAPS, 45*, 583-595. [16] Simon J. I. et al. (2005) *EPSL, 238*, 272-283. [17] Cosarinsky M. et al. (2005) *LPSC XXXVI*, Abstract #2105. [18] Taylor D. J. et al (2005) *LPSC XXXVI*, Abstract #2030. [19] Simon J. I. et al. (2011) *Science 331*, 1175 1178. [20] Bodénan J-D. et al. (2014) *EPSL, 401*, 327-336. [21] *Met. Bull. #103* (2014) in prep.